RESEARCH PAPER

Strontium Hexa-ferrites and Polyaniline Nanocomposite: Studies of Magnetization, Coercivity, Morphology and Microwave Absorption

Ardeshir Bagheri[1], Hamed Halakouie[2,], Davood Ghanbari[3], Mahdi Mousayi[2], Nakisa Asiabani[4]*

[1] Department of Physics, Faculty of Science, Imam Hossein University, Tehran, Iran

[2] Young Researchers and Elite Club, Arak Branch, Islamic Azad University, Arak, Iran

[3] Department of Science, Arak University of Technology, Arak, Iran

[4] Department of Physics, Faculty of Science, Arak University, Iran

ARTICLE INFO

ABSTRACT

In this work, the investigation of wave absorption, phase formation, crystal structure and magnetic properties of $SrFe_{12}O_{19}$ hexa-ferrites nanoparticles that synthesized by co-precipitation using a microwave heating system and polyaniline-$SrFe_{12}O_{19}$ was carried out by using a combination of vector network analyser (VNA), X-ray diffraction (XRD), scanning electron microscopy (SEM), and Fourier transform infrared (FT-IR) spectroscopy. Alternating gradient force magnetometer proofs the magnetic property of the hexa-ferrite nanostructures. We studied Sr Hexa-ferrite nanoparticles and nanocomposite by changing in many parameters like power of microwave system and calcination temperature.

INTRODUCTION

Microwave absorption materials have attracted much attention not only because of the military countermeasure to radar detection but also because of the intense demands for reduction of electromagnetic (EM) pollution/radiation and shielding interference in electric communication field [1–3]. Recently, many new techniques have been developed to synthesize microwave absorption materials with combination properties as high absorption rate, light weight, wide absorption band, anti-abrasion and low cost [4–6]. M-type strontium hexaferrites $SrFe_{12}O_{19}$ is currently a magnetic material with great scientific and technological interest, and has been widely used for permanent magnets, magnetic recording media, and microwave absorbers, due to its high stability, excellent high-frequency response, large magneto-crystalline anisotropy, and large magnetization as well [7-8]. In recent years, M-type hexagonal ferrite has displayed a promising application in microwave absorption due to their permittivity and permeability losses in the microwave frequency band [9-14]. Several techniques like chemical co-precipitation, solid-state reaction, sol–gel, hydrothermal, micro-emulsion method etc have been employed to prepare $SrFe_{12}O_{19}$ powders of different shapes and sizes. In this study, Strontium hexaferrites synthesised by microwave assisted method. Microwave systems provide the opportunity to complete reactions in minutes, and have manifold applications in academic and industrial environments alike. There are some important parameters in microwave synthesis such as choosing solvent, kind of reactions, heating

* Corresponding Author Email: h.halakouie@gmail.com

time and microwave power which can affect on synthesized products [15-17].

Currently, an increasing number of reports are focusing on synthesizing electromagnetic polyaniline (PANI)-based composites, conductive and magnetic materials such as ferrite, carbon nanotubes, graphene and nano-metals are always added in them [18]. PANI has been extensively studied due to its easy synthesis, low cost, excellent environmental stability and high electrical conductivity [19].

MATERIALS AND METHODS

$Sr(NO_3)_2$, $Fe(NO_3)_3$ $9H_2O$, NaOH, ethylene glycol, $C_6H_5NH_2$, Ammonium persulfate (APS) ($(NH_4)_2S_2O_8$) and Sodium dodecyl sulfate(SDS) were purchased from Merck and all the chemicals were used as received without further purifications. A multiwave ultrasonic generator (Bandeline MS 73), equipped with a converter/transducer and titanium oscillator, operating at 20 kHz with a maximum power output of 150 W was used for the ultrasonic irradiation. Room temperature magnetic properties were investigated using an alternating gradient force magnetometer (AGFM) device, made by Meghnatis Kavir Kashan Company (Iran) in an applied magnetic field sweeping between ±10000 Oe. XRD patterns were recorded by a Philips, X-ray diffractometer using Ni-filtered CuK_α radiation. SEM images were obtained using

a LEO instrument model 1455VP. Prior to taking images, the samples were coated by a very thin layer of Pt (using a BAL-TEC SCD 005 sputter coater) to make the sample surface conductor and prevent charge accumulation, and obtaining a better contrast.

Synthesis of $SrFe_{12}O_{19}$ nanoparticles

0.012 mole of $Fe(NO_3)_3$ $9H_2O$ and 0.001 mole of $Sr(NO_3)_2$ were dissolved in 100 ml (or 200 ml) of ethylene glycol and put under microwave with 170, 510 and 850 W. 35 ml of NaOH solution (1M) was then slowly added to the solution until reaching pH to around 10. A brown precipitate was then centrifuged and rinsed with distilled water. Finally the obtained precipitate was calcinated at 550-850 °C and its colour goes from brown to black. Fig. 1 shows the schematic diagram for experimental setup for nanoparticles preparation used in the microwave process.

Synthesis of PANI and $SrFe_{12}O_{19}$ nanocomposite

1.1 gr Aniline monomer, 1 gr Sr nanoparticles and 5 gr SDS added to 10 ml distilled water. In order to improve the contacts between the ferrites and anilines in the aqueous solution, nano-sized ferrites were dispersed in deionized water by ultrasonic waves for 30 min before polymerization. 2.28 g APS in 10 ml distilled water was added to the solution at the same time. Then the required
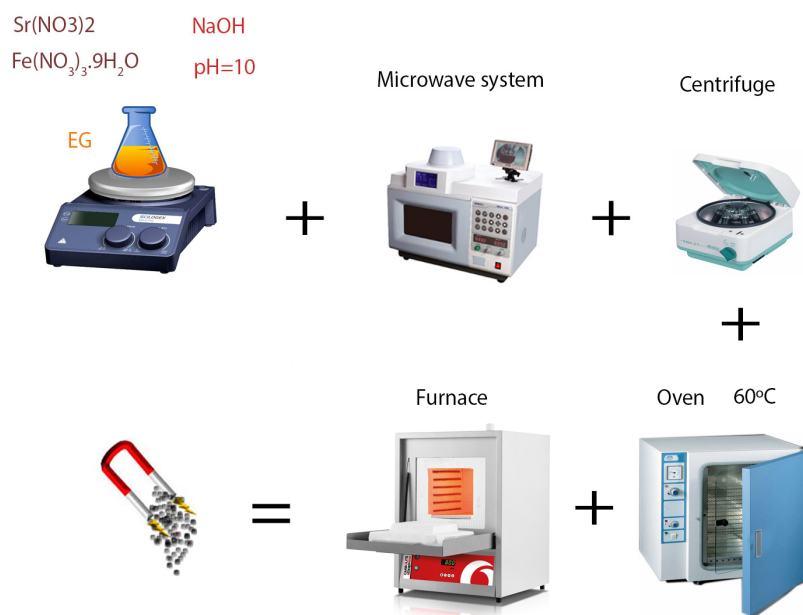

Fig. 1. Schematic of Sr hexa-ferrite preparation

amount of aniline was placed in the flask, and the polymerization was allowed to proceed at a temperature between 0 and 4 °C under stirring for 5h. A dark green precipitate was then obtained and rinsed with distilled water. Finally, the products were dried in at room temperature.

RESULTS AND DISCUSSION

The structure and composition of the $SrFe_{12}O_{19}$ nanoparticles were investigated. Fig. 2 shows XRD pattern of a sample including $SrFe_{12}O_{19}$ nanoparticles that prepared in 510 W and 850 °C. The result reveals the typical diffraction patterns of pure hexagonal phase (JCPDS No.: 24-1207) with

P63-mmc space group which is consistent with pure Sr hexa-ferrite. The crystalline size of product was calculated using Scherrer equation i.e. $Dc=K\lambda/\beta Cos\theta$, where β is the width of the observed diffraction peak at its half maximum intensity (FWHM), K is the shape factor, which takes a value of about 0.9, and λ is the X-ray wavelength (CuKα radiation, equals to 0.154 nm). The average crystalline size for SrFe12O19 nanoparticles was found to be about 15 nm.

In order to investigate the effect of microwave power on the morphology of the Sr hexa-ferrites scanning electron microscopy employed (all samples prepared in 10 microwave pulses(5
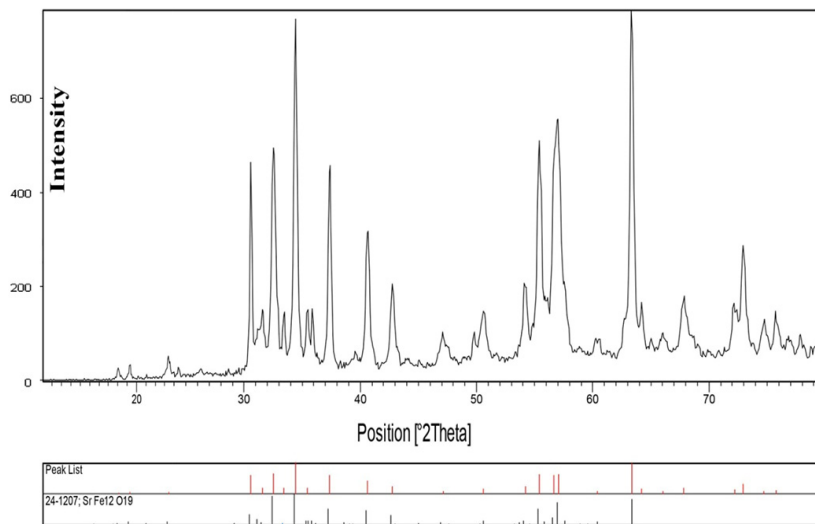

Fig. 2. XRD pattern of Sr hexa-ferrite nanoparticles at 510W and 850 °C (10 pulses)
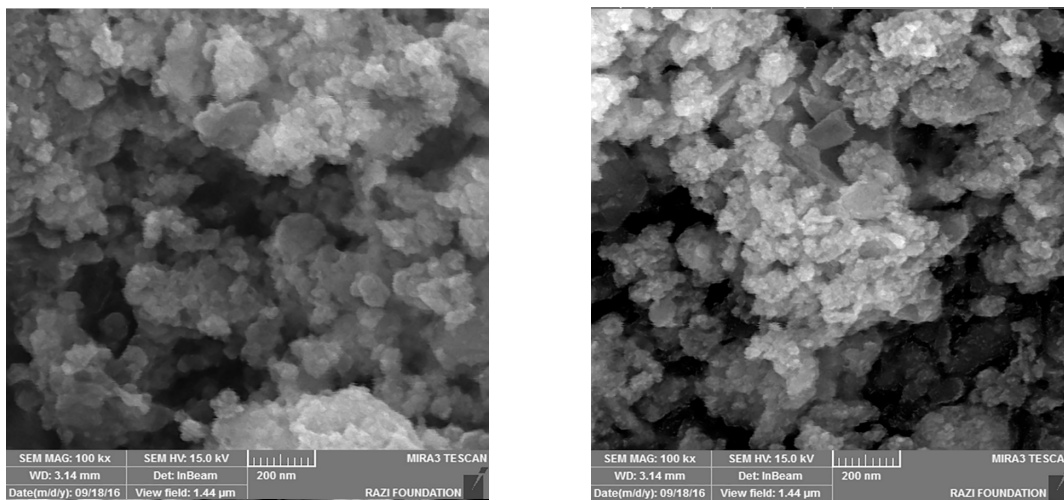

Fig. 3. SEM images of Sr hexa-ferrite at 170W and 850 °C (10 pulses)

minutes)). Figs. 3 illustrate SEM images of the as-synthesized Sr hexa-ferrites nanoparticles obtained at microwave power 170 W and calcination 850 ℃. The results confirm that synthesized nanostructures are formed from nanoparticles with average diameter size less than 100 nm. In power 170 inhomogeneous particle were grown, Because little energy has reached to the solution during the preparation, growth stage has overcome nucleation, and particles grow through the way they have lower energy.

Fig. 4 shows the SEM micrographic of Sr hexa-ferrite samples produced at 510W and 850 ºC. it confirms the formation of homogeneous morphology in spherical with uniformly dispersed

nanometer. It seems nucleation preferential compare to the crystal growth. The average particle size is found to be around 70 nm.

Figs. 5 give SEM images of Sr hexa-ferrite that achieved at 850 W. The average particle size is found to be around 80 nm indicating; the sheet shape nanoparticles that achieved by increasing microwave power.

The effect of calcination temperature on the morphology of samples was also examined. We saw at lower and higher powers have larger particles size compare with which prepare at moderate microwave power (510 W). Fig. 6 show SEM images of the prepared samples at power 510 W and calcination 550℃. Fig. 6 show the same
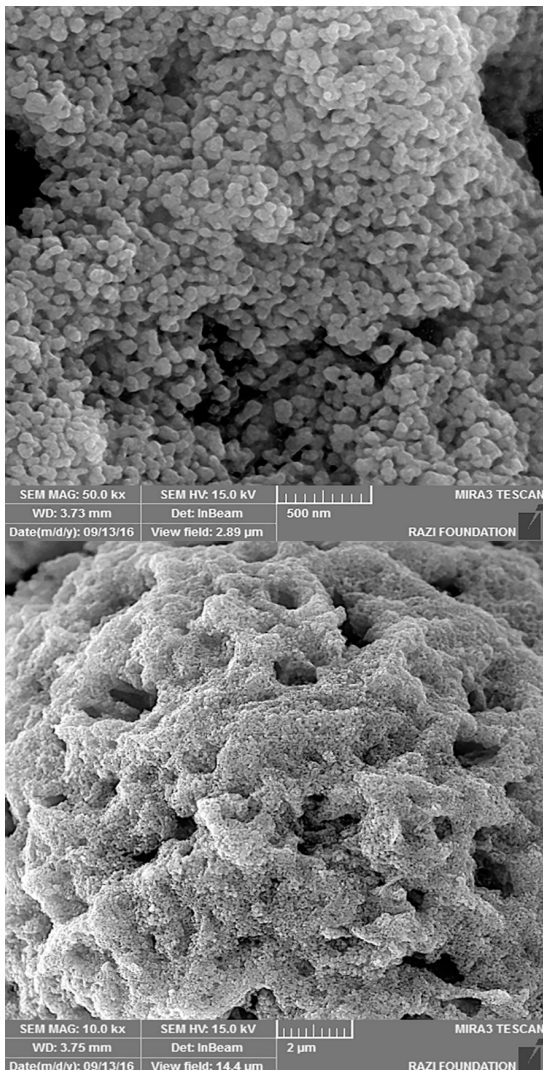

Fig. 4. SEM images of Sr hexa-ferrite at 510W and 850℃ (10 pulses)

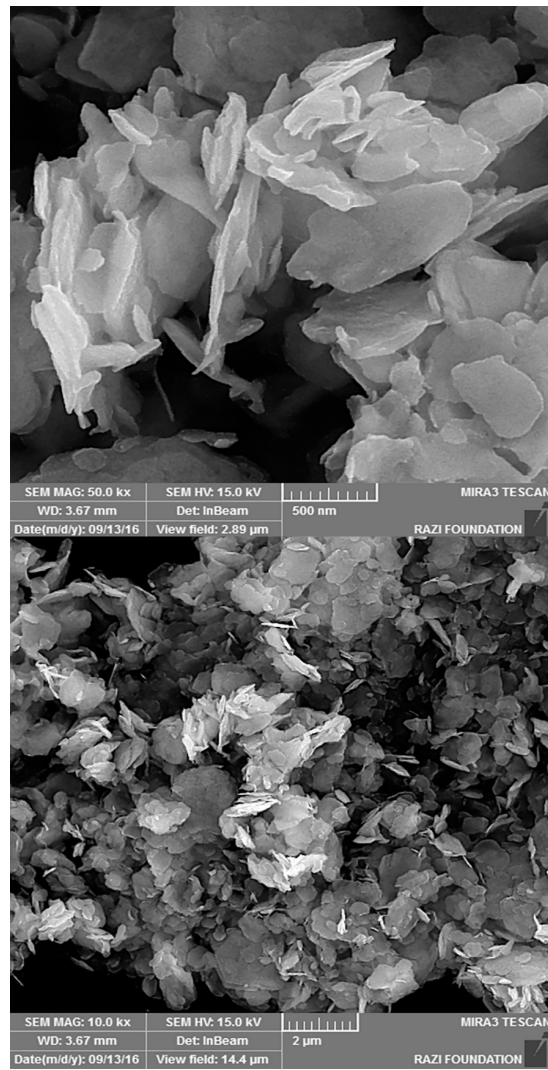
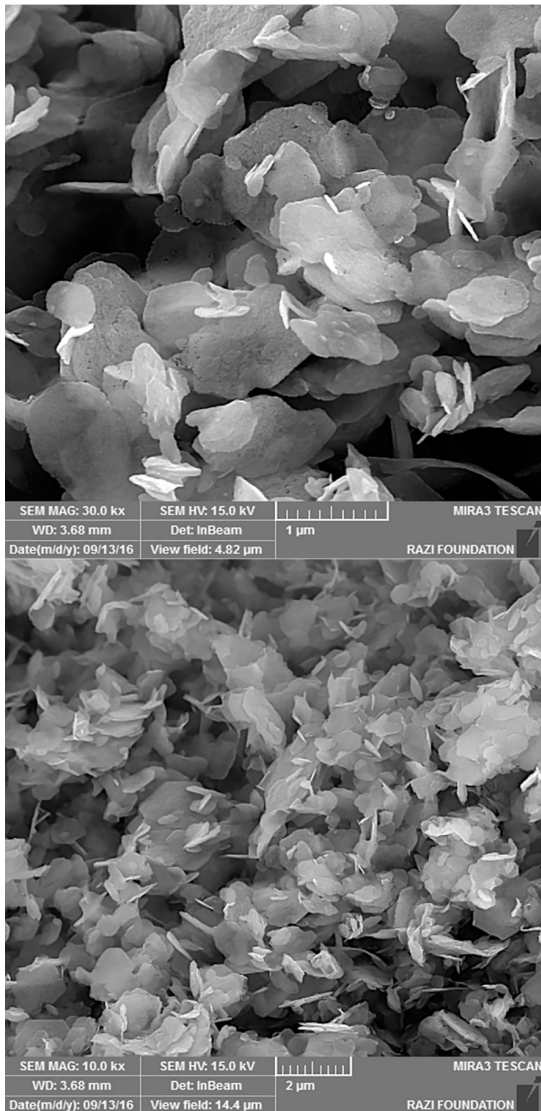Fig. 5. SEM images of Sr hexa-ferrite at 850W and 850℃ (10 pulses)

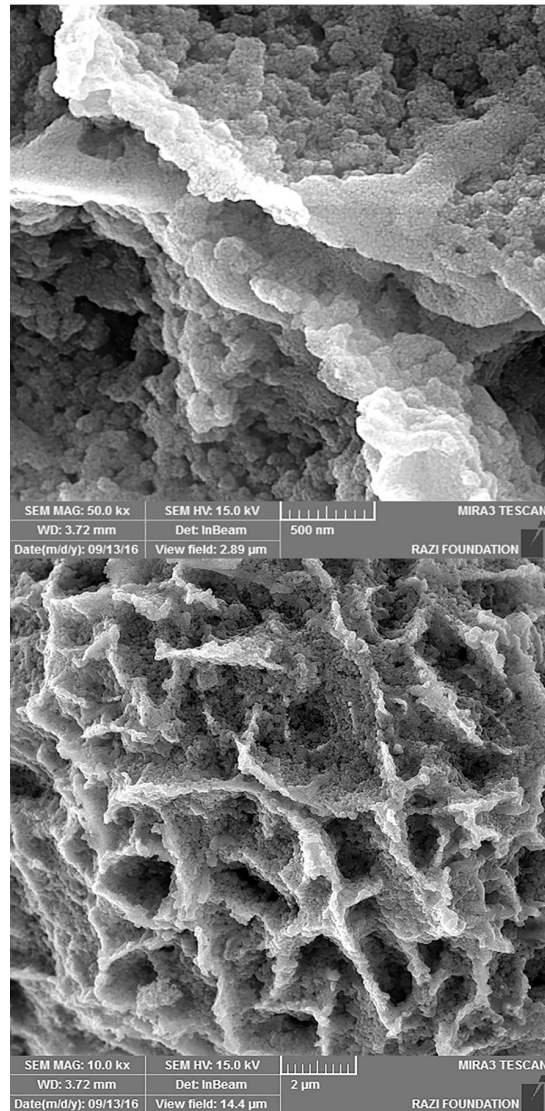Fig. 6. SEM images of Sr hexa-ferrite at 510W and 550°C (10 pulses)

Fig. 7. SEM images of Sr hexa-ferrite at 510W and 700°C (10 pulses)

nanostructural characteratics like fig.5. Fig. 7 show SEM images of Samples obtained at power 510 W and calcination 700°C and reveals that in this condition, mono-disperse product with mediocre size of around 50 nm was synthesized. Microwave proposes fast manipulation in particle size, so different magnetic properties are obtained by a simple change in power and temperature. Fig. 8 shows SEM images of polyaniline and Sr hexa-ferrite nanocomposite. The results show that a continuous overlayer of conducting polymers is produced on the ferrite particle surface. Since the balance between nucleation and growth rates, determines final particle size of products,

thus the morphology of products depends on the preparation conditions.

Hysteresis loop for Sr hexa-ferrite nanoparticles with calcination temperature of 850°C is shown in Fig. 9 Coercivity and saturation magnetization of this sample is about 5200 Oe and 33 emu/g respectively. Fig. 10 shows hysteresis curve of Sr hexa-ferrite prepared at 550°C that exhibits ferromagnetic behaviour with a coercivity of 3100 Oe and saturation magnetization of 20 emu/g. Interestingly it was observed at low calcination temperature coercivity is much less than which prepared at 850° C. The outcomes indicate the existence of direct effect of morphology and
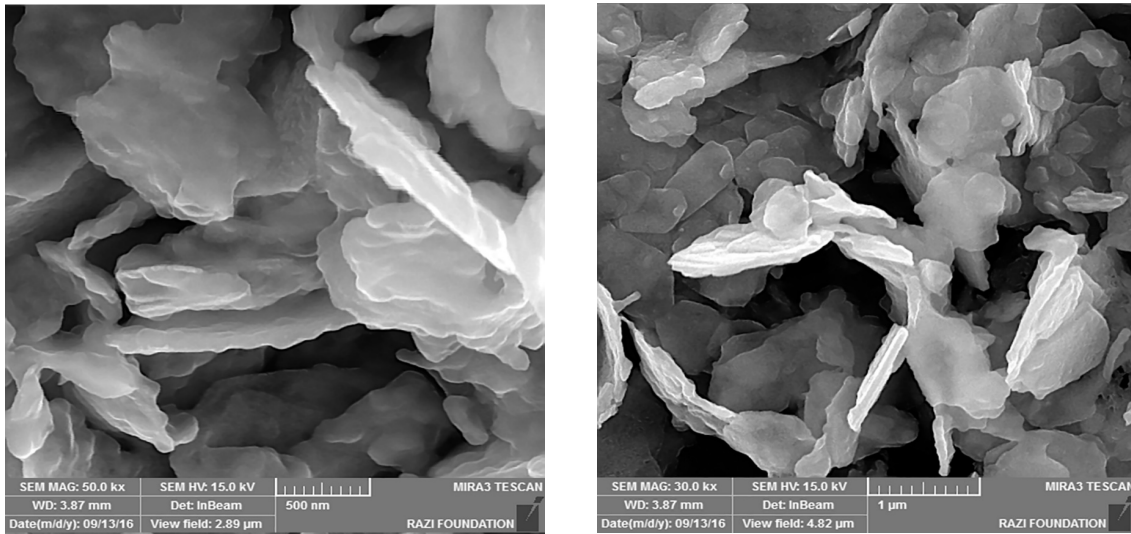
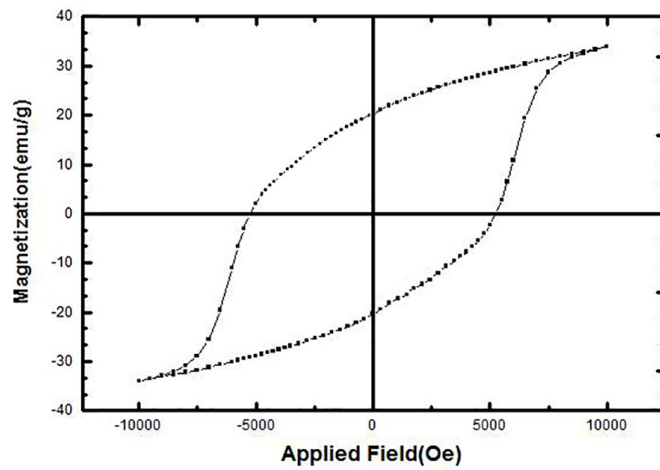Fig. 8. SEM images of polyaniline and Sr hexa-ferrite nanocomposite

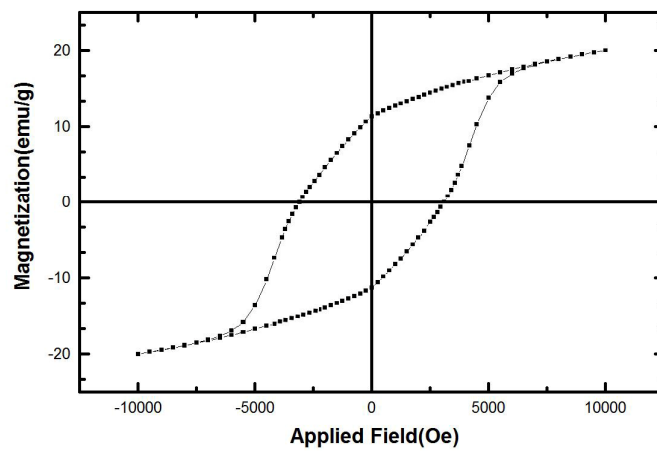Fig. 9. AGFM analysis of Sr hexa-ferrite at 510W and 850°C (10 pulses)

Fig. 10. AGFM analysis of Sr hexa-ferrite at 510W and 550°C (10 pulses)

Fig. 11. AGFM analysis of polyaniline and Sr hexa-ferrite

Fig. 12. FT-IR of Sr hexa-ferrite at 510W and 850°C

particle size on the magnetic property of the prepared ferrite. For investigate effect of power on magnetic properties Fig. 11 shows magnetization curve of polyaniline and Sr hexa-ferrite nanocomposite that also exhibits ferromagnetic behaviour with a coercivity of about 4000 Oe and saturation magnetization of 17 emu/g.

Fig. 12 Shows the FT-IR spectrum of the prepared Sr hexa-ferrite nanoparticles at temperature of 850 °C. The absorption bands at 447 and 601 cm^{-1} are assigned to the stretching mode of Fe-O and Sr-O bonds. FT-IR spectrum of nanoparticles clearly shows that the metal-oxygen bonds are present in

the spectrum. It exhibits a broad absorption peak between 3200-3600 cm^{-1}, corresponds to the stretching mode of O-H group of hydroxyl group. A little amount of precursors were remained at surface of nanoparticles at 850°C and responsible peaks exist in 1400-1600 cm^{-1} .FT-IR spectrum of the polyaniline and SrFe$_{12}$O$_{19}$ nanocomposite is shown in Fig. 13 A strong absorptions band at 408 and 588 cm^{-1} which approve presence of SrFe$_{12}$O$_{19}$ magnetic nanoparticles is clearly observed. Peaks at 1710 cm^{-1} is related to C=N bond and peaks at 1400-1600 cm^{-1} are responsible to C-C and C=C bonds. Absorption around 1200-1302
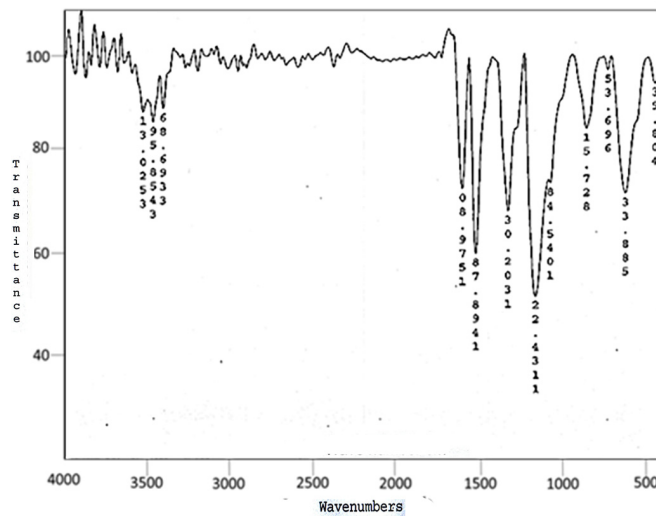
636

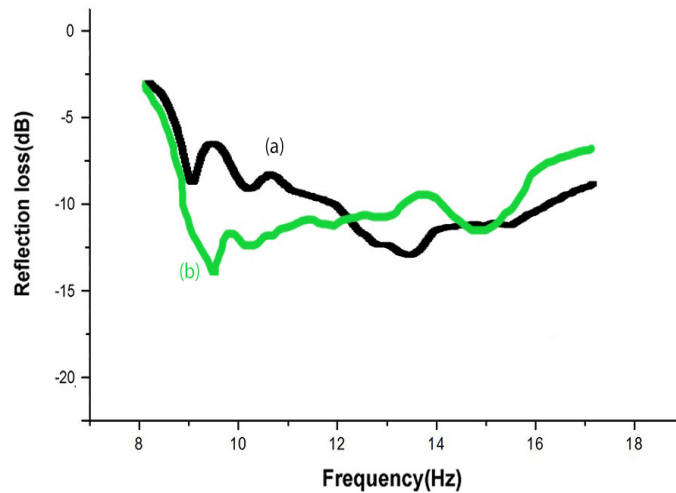Fig. 13. FT-IR of polyaniline and Sr hexa-ferrite nanocomposite

Fig. 14. Variation of reflection loss vs. frequency of a) Sr hexa-ferrite and b) PANI-Sr hexa-ferrite nanocomposite

cm^{-1} is related to N–H bending and asymmetric C–N stretching modes of the benzenoid ring, The strong peak around 1134 cm^{-1} is associated with vibration modes of N = Q = N (Q refers to the quinonic type rings), indicating that PANI polymer is formed in nanocomposite.

The specimens for microwave adsorption testing were prepared by homogeneously mixing the composite powders with 20 wt% paraffin Fig. 14 presents the variation of reflection loss and frequency for the $SrFe_{12}O_{19}$ nanoparticles and PANI- $SrFe_{12}O_{19}$ nanocomposite. It can be seen that PANI- $SrFe_{12}O_{19}$ nanocomposite have more obvious effect on microwave-absorbing properties than $SrFe_{12}O_{19}$ nanoparticles. There is less difference in

relection loss between 12-17 GH. PANI-$SrFe_{12}O_{19}$ demonstrated a microwave absorbing band-wide between 9.2 and 9.8 GHz, where reflections observed on a network analyzer lost from -8.7 to -15 dB.

CONCLUSIONS

In conclusion, synthesis, characterization of $SrFe_{12}O_{19}$ nanoparticles reported. Effect of calcination temperature and microwave power on the morphology and particle size of the products was investigated. indicating; the particle size and the nanoparticles' morphology can be easily controlled by this parameters. AGFM results confirm that the synthesized nanoparticles exhibit

ferromagnetic behaviour. However, increasing power and temperature leads to increase of coercivity. Also PANI-SrFe$_{12}$O$_{19}$ nanocomposite was successfully synthesized by the facile oxidative chemical polymerization of aniline in the presence of SrFe$_{12}$O$_{19}$ nanoparticles. The PANI-SrFe$_{12}$O$_{19}$ nanocomposite have stronger absorption for microwave between 8.0 and 12.0 GHz than pure hexagonal ferrite.

CONFLICT OF INTEREST

The authors declare that there are no conflicts of interest regarding the publication of this manuscript.

REFERENCES

1. Khairy M. Synthesis, characterization, magnetic and electrical properties of polyaniline/NiFe2O4 nanocomposite. Synthetic Metals. 2014;189:34-41.

2. Khademi F, Poorbafrani A, Kameli P, Salamati H. Structural, Magnetic and Microwave Properties of Eu-doped Barium Hexaferrite Powders. Journal of Superconductivity and Novel Magnetism. 2011;25(2):525-31.

3. Wang T, Wang H, Chi X, Li R, Wang J. Synthesis and microwave absorption properties of Fe–C nanofibers by electrospinning with disperse Fe nanoparticles parceled by carbon. Carbon. 2014;74:312-8.

4. Cheng JH, Tian CA. Preparation and electrochemical properties of perovskite CexLi0.5-xCa0.5TiO3composites. IOP Conference Series: Materials Science and Engineering. 2018;292:012016.

5. Hosseini SH, Moghimi A, Moloudi M. Magnetic, conductive, and microwave absorption properties of polythiophene nanofibers layered on MnFe2O4/Fe3O4 core–shell structures. Materials Science in Semiconductor Processing. 2014;24:272-7.

6. Zhan J, Yao Y, Zhang C, Li C. Synthesis and microwave absorbing properties of quasione-dimensional mesoporous NiCo2O4 nanostructure. Journal of Alloys and Compounds. 2014;585:240-4.

7. Wang JF, Ponton CB, Harris IR. A study of Sm-substituted SrM magnets sintered using hydrothermally synthesised powders. Journal of Magnetism and Magnetic Materials. 2006;298(2):122-31.

8. Haijun Z, Zhichao L, Chengliang M, Xi Y, Liangying Z, Mingzhong W. Complex permittivity, permeability, and microwave absorption of Zn- and Ti-substituted barium ferrite by citrate sol–gel process. Materials Science and Engineering: B. 2002;96(3):289-95.

9. Yuan CL, Hong YS. Microwave adsorption of core–shell structure polyaniline/SrFe12O19 composites. Journal of Materials Science. 2010;45(13):3470-6.

10. Huang Y, Li Y, Wang Y. Magnetic and electromagnetic properties of Pr doped strontium ferrite/polyaniline composite film. Journal of Magnetism and Magnetic Materials. 2014;368:133-8.

11. Ghanbari D, Salavati-Niasari M. Hydrothermal synthesis of different morphologies of MgFe2O4 and magnetic cellulose acetate nanocomposite. Korean Journal of Chemical Engineering. 2015;32(5):903-10.

12. Ghanbari D, Salavati-Niasari M, Ghasemi-Kooch M. A sonochemical method for synthesis of Fe3O4 nanoparticles and thermal stable PVA-based magnetic nanocomposite. Journal of Industrial and Engineering Chemistry. 2014;20(6):3970-4.

13. Ghanbari D, Salavati-Niasari M. Synthesis of urchin-like CdS-Fe3O4 nanocomposite and its application in flame retardancy of magnetic cellulose acetate. Journal of Industrial and Engineering Chemistry. 2015;24:284-92.

14. Ghanbari D, Salavati-Niasari M, Ghasemi-Kooch M. In situ and ex situ synthesis of poly(vinyl alcohol)–Fe3O4 nanocomposite flame retardants. Particuology. 2016;26:87-94.

15. Zhu Y-J, Chen F. Microwave-Assisted Preparation of Inorganic Nanostructures in Liquid Phase. Chemical Reviews. 2014;114(12):6462-555.

16. Microwaves in Nanoparticle Synthesis. Wiley-VCH Verlag GmbH & Co. KGaA; 2013.

17. Shinohara N. Power without wires. IEEE Microwave Magazine. 2011;12(7):S64-S73.

18. Qazi TH, Rai R, Boccaccini AR. Tissue engineering of electrically responsive tissues using polyaniline based polymers: A review. Biomaterials. 2014;35(33):9068-86.

19. Zhu Y-F, Ni Q-Q, Fu Y-Q, Natsuki T. Synthesis and microwave absorption properties of electromagnetic functionalized Fe3O4–polyaniline hollow sphere nanocomposites produced by electrostatic self-assembly. Journal of Nanoparticle Research. 2013;15(10).